

# Inhibition of cell proliferation through an ATP-responsive co-delivery system of doxorubicin and Bcl-2 siRNA

Jianxu Zhang<sup>1,2,\*</sup>Yudi Wang<sup>2,\*</sup>Jiawen Chen<sup>2</sup>Xiao Liang<sup>2</sup>Haobo Han<sup>1,2</sup>Yan Yang<sup>2</sup>Quanshun Li<sup>1,2</sup>Yanbo Wang<sup>1</sup>

<sup>1</sup>Department of Urology, First Hospital of Jilin University, <sup>2</sup>Key Laboratory for Molecular Enzymology and Engineering of Ministry of Education, School of Life Sciences, Jilin University, Changchun, People's Republic of China

\*These authors contributed equally to the work

**Abstract:** Herein, DNA duplex was constructed through the hybridization of adenosine triphosphate (ATP)-responsive aptamer and its cDNA in which GC-rich motif could be used to load doxorubicin (DOX), and then, cationic polymer PEI25K was used as a carrier to simultaneously condense DOX-Duplex and Bcl-2 siRNA to prepare the ternary nanocomplex polyethylenimine (PEI)/DOX-Duplex/siRNA. The ATP concentration gradient between the cytosol and extracellular environment could achieve the stable loading of DOX in duplex and the rapid drug release in an ATP-responsive manner. Using human prostate tumor cell line PC-3 as a model, an obvious induction of cell proliferation could be detected with a cell viability of 53.3%, which was stronger than single cargo delivery, indicating the synergistic effect between these two components. The enhanced anti-proliferative effect of ternary nanocomplex could be attributed to the improved induction of cell apoptosis in a mitochondria-mediated pathway and cell-cycle arrest at the G2 phase. Overall, the ATP-responsive nanocarrier for co-delivering DOX and Bcl-2 siRNA has been demonstrated to be a smart delivery system with favorable anti-proliferative effect, especially for solving the multidrug resistance of tumors.

**Keywords:** ATP response, aptamer, doxorubicin, Bcl-2 siRNA, anti-proliferation, synergistic effect

## Introduction

In the cancer treatment, chemotherapy still plays an important role despite great advances in the field of surgery and radiotherapy.<sup>1</sup> However, an important limitation associated with chemotherapy is the emergence of multidrug resistance,<sup>2,3</sup> which can be divided into two types, pump and non-pump resistance.<sup>4</sup> The pump resistance is caused by drug efflux pumps on the cell membrane, which decrease the intracellular concentration of drugs and ultimately lead to the failure of chemotherapy,<sup>5-7</sup> while the non-pump resistance is based on the anti-apoptotic defense, which enables the cancer cells to survive against the chemotherapeutics.<sup>8-10</sup> The Bcl-2 protein has been considered to be a key executor for non-pump resistance, which can inhibit the release of cytochrome C after the initiation of apoptosis and block the downstream propagation of death signal, thereby promoting the cell survival.<sup>11</sup> Previous research has shown that decreasing the expression level of Bcl-2 by the siRNA technique could efficiently trigger the apoptosis of cancer cells.<sup>12,13</sup> More importantly, the combination of chemotherapy and gene therapy such as Bcl-2 siRNA has been demonstrated to enhance the efficacy and improve the therapeutic outcome,<sup>14-17</sup> owing to the synergistic anticancer activity or enhanced sensitivity to chemotherapeutics.

Correspondence: Quanshun Li; Yanbo Wang  
Department of Urology, First Hospital of Jilin University, Changchun 130012, People's Republic of China  
Tel +86 431 8515 5381  
Fax +86 431 8515 5200  
Email quanshun@jlu.edu.cn; doctorwyb@126.com

Up to now, the co-delivery of chemotherapeutic agents and siRNA mediated by nanocarriers has been demonstrated to be effective in both in vitro and in vivo studies.<sup>18</sup> To further enhance the biological specificity and therapeutic efficacy, great efforts have been devoted to construct stimuli-responsive delivery systems, which can improve the accumulation of nanocarriers at tumor sites and rapidly release the payloads within tumor cells.<sup>19</sup> External signals such as magnetic field, light and temperature or internal ones such as pH, redox potential and enzymatic activities have been widely used to construct stimuli-responsive nanocarriers for improving the drug delivery efficiency.<sup>20,21</sup> However, complex design processes and accurate experimental conditions could not be avoided in the construction of these stimuli-responsive nanocarriers.<sup>21</sup> Thus, it is still of great challenge to explore more facial and efficient stimuli-responsive nanocarriers, especially for achieving the co-delivery of drug and gene. Recently, adenosine triphosphate (ATP)-responsive nanocarriers for co-delivering drugs and genes have been successfully developed,<sup>20–27</sup> based on the higher ATP concentration in the intracellular fluids (1–10 mM) than in the extracellular environment (<0.4 mM).<sup>28,29</sup> For instance, Mo et al<sup>20</sup> constructed an ATP-triggered nanocarrier for doxorubicin (DOX) release through an ATP-responsive duplex (the ATP aptamer and its complementary single-stranded DNA), whose GC-rich motif was used to intercalate DOX into the aptamer duplex. In an ATP-rich condition, ATP molecules will trigger the rapid release of DOX and high anti-proliferative effect owing to the dissociation of aptamer duplex.

In the present research, an ATP-triggered nanosystem for achieving the co-delivery of DOX and Bcl-2 siRNA was constructed based on an ATP-responsive aptamer duplex, in which the rapid release of DOX and Bcl-2 siRNA could be achieved under ATP-rich conditions. Then, the nanosystem-mediated inhibition of cell proliferation was systematically evaluated, including cell apoptosis and cell-cycle arrest, using human prostate tumor cell line PC-3 as a model.

## Materials and methods

### Materials

DOX in the form of hydrochloride salt (>99%) was purchased from Huafeng Biotech. Co. (Beijing, People's Republic of China) and used as received. Bcl-2 siRNA (sense: 5'-UGU GGA UGA CUG AGU ACC UGA dTdT-3'; antisense: 5'-UCA GGU ACU CAG UCA UCC ACA dTdT-3') and 5-carboxyfluorescein (FAM)-labeled Bcl-2 siRNA (FAM-siRNA) was synthesized by GenePharma (Suzhou, People's Republic of China). ATP-responsive aptamer (5'-ACC TGG GGG AGT ATT GCG GAG GAA

GGT-3') and its cDNA (5'-ACC TTC CTC CGC AAT ACT CCC CCA GGT-3') were synthesized by Sangon Biotech (Shanghai, People's Republic of China). Polyethylenimine (PEI) with a molecular weight of 25 kDa (PEI25K) was obtained from Sigma-Aldrich Co. (St Louis, MO, USA). Dulbecco's Modified Eagle's Medium (DMEM) and fetal bovine serum (FBS) were purchased from Thermo Fisher Scientific (Waltham, MA, USA). 3-(4,5-Dimethylthiazol-2-yl)-2,5-diphenyltetrazolium bromide (MTT) was purchased from Amersco (Solon, OH, USA). Diethyl pyrocarbonate (DEPC)-treated water, biconchonic acid (BCA) protein assay kit and 4',6-diamidino-2-phenylindole (DAPI) were obtained from DingGuo Biotech. Co. (Beijing, People's Republic of China). LIVE/DEAD® Viability/Cytotoxicity kit was purchased from Thermo Fisher Scientific. Annexin V-fluoresceine isothiocyanate (FITC)/PI apoptosis detection kit, cell-cycle detection kit and caspase-3, -8 and -9 activity assay kits were purchased from Bestbio (Shanghai, People's Republic of China). Polyvinylidene fluoride (PVDF) membrane was purchased from EMD Millipore (Billerica, MA, USA). Antibodies against  $\beta$ -actin, Bcl-2, procaspase-3 and horseradish peroxidase (HRP)-labeled goat anti-mouse IgG were purchased from Abcam (Cambridge, UK).

### Construction and characterization of PEI/DOX-Duplex/siRNA nanocomplex

The ATP aptamer and its cDNA were first dissolved in DEPC-treated water to achieve a concentration of 20  $\mu$ M. Then, these two solutions (160  $\mu$ L) were mixed together and incubated at room temperature for 15 min to obtain duplex, into which 320  $\mu$ L of DOX solution (20  $\mu$ M in DEPC-treated water) was added. The mixture was incubated at room temperature for another 15 min to construct DOX-Duplex. Bcl-2 siRNA solution (0.264  $\mu$ g/ $\mu$ L in DEPC-treated water) was mixed with DOX-Duplex in different ratios, and PEI25K was added into the mixture at predetermined mass ratios. The sample was incubated at room temperature for 30 min to obtain PEI/DOX-Duplex/siRNA nanocomplex.

The DOX loading was monitored by comparing the fluorescence spectra of DOX solution (320  $\mu$ L, 20  $\mu$ M) and DOX-Duplex solution, both of which were diluted to 3 mL using DEPC-treated water before detection. The ATP-triggered DOX release was detected by observing the fluorescence intensity changes of DOX-Duplex treated with different concentrations of ATP (0, 0.4 and 4.0 mM) in the dark for 15 min. The fluorescence spectra were performed on the Shimadzu RF-5301 fluorescence spectrometer (Kyoto, Japan) with excitation and emission wavelengths of 480 and 500–700 nm,

respectively. The condensation of PEI25K for DOX-Duplex and Bcl-2 siRNA and the nanocomplex stability in the serum were detected by gel retardation assay. The nanocomplex was incubated at 37°C for 3 h in the presence or absence of 50% FBS and analyzed by 1% agarose gel electrophoresis in Tris-acetate-EDTA (TAE) buffer (120 V, 20 min). The particle size and zeta potential of nanocomplex were determined by Malvern Nano ZS90 Zetasizer (Malvern Instruments, Malvern, UK).

### Cellular uptake of PEI/DOX-Duplex/siRNA

The PC-3 cells were obtained from the Shanghai Institute of Cell Bank (Shanghai, People's Republic of China) and cultured in DMEM supplemented with 100 IU/mL penicillin, 100 mg/mL streptomycin and 10% FBS at 37°C in a humidified atmosphere of 5% CO<sub>2</sub>. For cellular uptake assay, the cells were cultured in six-well plates at 37°C for 24 h at an initial density of 3.0×10<sup>5</sup> cells/well, treated with PEI/DOX-Duplex/siRNA for 6 h and observed through IX71 fluorescence microscopy (Olympus Corporation, Tokyo, Japan). In addition, the intracellular DOX release was monitored at different incubation times.

### Inhibition of cell proliferation by PEI/DOX-Duplex/siRNA

The inhibition of cell proliferation mediated by PEI/DOX-Duplex/siRNA was evaluated by the MTT assay. Briefly, PC-3 cells were seeded in 96-well plates at a density of 8.0×10<sup>3</sup> cells/well and cultured to 80% confluence. Then, the medium was removed from each well, and 200 μL of FBS-free DMEM containing different nanocomplexes (10 μg/mL PEI25K, 5 μg/mL DOX-Duplex and 15 μg/mL siRNA) was added into the wells. After 24 h treatment, the cells in each well were incubated with 20 μL of MTT solution (5 mg/mL in PBS) for an additional 4 h. The formed formazan crystals were dissolved by 150 μL dimethyl sulfoxide (DMSO) for 10 min after removing the MTT solution. The cell viability was calculated as the ratio of absorbance values at 492 nm of treatment and control groups, which were measured by the GF-M3000 microplate reader (Caihong Corporation, Shandong, People's Republic of China). Additionally, Live/Dead staining was conducted in six-well plates to directly observe the induction of cell proliferation induced by nanocomplex. The cells were cultured in an initial density of 2.0×10<sup>5</sup> cells/well, and the treatment was carried out using nanocomplex with the same DOX or siRNA concentration as the MTT assay. Then, the cells were stained with live/dead reagents for 20 min according to the manufacturer's

instructions, washed with PBS twice and observed through IX71 fluorescence microscopy (Olympus Corporation).

### Induction of cell apoptosis by PEI/DOX-Duplex/siRNA

Briefly, PC-3 cells were seeded in six-well plates at a density of 2.0×10<sup>5</sup> cells/well and cultured at 37°C for 24 h before transfection. As described earlier, the cells were treated with different nanocomplexes in 2 mL of FBS-free DMEM for 24 h, with DOX-Duplex and siRNA concentrations of 5 and 15 μg/mL, respectively. According to the protocol provided in Annexin V-FITC/PI apoptosis detection kit, the harvested cells were washed with PBS twice, re-suspended in binding buffer and incubated with Annexin V-FITC and propidium iodide (PI) solutions at room temperature for 10 min in the dark. Finally, the cell apoptosis was analyzed by FACSCalibur (BD Biosciences, San Jose, CA, USA) with 15,000 ungated cells used.

### Induction of cell-cycle arrest by PEI/DOX-Duplex/siRNA

The cell culture and PEI/DOX-Duplex/siRNA treatment were conducted as described in the cell apoptosis analysis. For cell-cycle assay, the harvested cells were first fixed in 70% ethanol at 4°C overnight and then washed with PBS twice and incubated with 20 μL of RNase A solution at 37°C for 30 min and 300 μL of PI solution at 4°C for 1 h in the dark. Finally, the cell cycle was measured by analyzing 15,000 ungated cells through FACSCalibur.

### Western blot assay

The cell culture and PEI/DOX-Duplex/siRNA treatment were conducted as described in the cell apoptosis analysis. Prior to Western blot analysis, PC-3 cells were collected, washed with PBS twice and treated with radioimmunoprecipitation assay (RIPA) lysis buffer on ice for 2 h. The supernatants were obtained through the centrifugation of lysates at 12,000 rpm for 10 min. After determining the protein concentration by BCA protein kit, SDS-PAGE following transfer to PVDF membrane via electroblotting was performed using an equal amount of proteins. The membrane was blocked in PBS containing 10% non-fat milk and 0.1% Tween-20 for 2 h and incubated with the primary antibodies (antibodies against β-actin, Bcl-2 and procaspase-3) at 4°C overnight. After washing with PBS containing 0.1% Tween-20 (PBST) three times, the membrane was treated with HRP-labeled secondary antibody at room temperature for 1 h and washed with PBST twice. Finally, the expression levels were normalized against β-actin and detected through enhanced

chemical luminescence (TransGen Biotech, Beijing, People's Republic of China).

### Caspase-3, -8 and -9 activities assay

The cell culture and PEI/DOX-Duplex/siRNA treatment were conducted as described in the cell apoptosis analysis, and caspase-3, -8 and -9 activities were assayed using the corresponding kits. After washing with PBS twice, the cells were further treated with 100  $\mu$ L lysis buffer, after which the supernatants were centrifuged at 10,000  $g$  for 10 min. Finally, 10  $\mu$ L supernatant was used to detect the caspase-3, -8 and -9 activities according to the manufacturer's instructions, in which the absorbance at 405 nm was recorded on the GF-M3000 microplate reader.

## Results and discussion

The duplex was first prepared through the hybridization of ATP aptamer and its cDNA, and its GC-rich motif could be used to load the antitumor agent DOX. To detect whether DOX was intercalated into the DNA duplex, the fluorescence spectra analysis of DOX and DOX-Duplex was conducted. As shown in Figure 1A, free DOX exhibited strong fluorescence absorption at 570 nm, while the fluorescence intensity of DOX-Duplex was dramatically reduced, which meant the successful loading of DOX in the duplex. The decreased fluorescence intensity was caused by the resonance energy transfer between DOX molecules when interacted into the DNA duplex.<sup>30,31</sup> In the present study, ATP-binding aptamer and its cDNA were used to construct the DNA duplex, and ATP molecules could specially recognize and activate the aptamer, which would directly promote the release of loaded DOX molecules. Thus, the ATP-triggered DOX release was then studied through the incubation of DOX-Duplex in the

presence of ATP at different concentrations (Figure 1B). A low concentration of ATP (0.4 mM) could not induce the DOX release as the fluorescence intensity was almost identical to that without ATP treatment. Nevertheless, a high ATP concentration (4.0 mM) could efficiently achieve the release of DOX, indicating the drug release in an ATP-responsive manner. The ATP concentration exhibited a significant difference between the intracellular fluids (1–10 mM) and extracellular environment (<0.4 mM).<sup>28,29</sup> Thus, the ATP concentration gradient could be used for realizing the stable loading of DOX in the DNA duplex and the rapid drug release in the cytosol, and these characteristics made it probably an ideal smart delivery system.

The ATP-responsive co-delivery system was then constructed through the incubation of PEI25K, DOX-Duplex and Bcl-2 siRNA at room temperature for 30 min, namely PEI/DOX-Duplex/siRNA. The cationic carrier PEI25K has been demonstrated to possess superior gene transfection efficiency both in vitro and in vivo, as its high positive charge and proton-buffering capacity can condense nucleic acids to form stable nanocomplex, protect them from the degradation in the serum and facilitate the efficient cellular uptake and rapid release from endosomes.<sup>32,33</sup> Agarose gel electrophoresis was conducted to detect the condensation ability of PEI25K with DOX-Duplex and siRNA. As shown in Figure 2A, PEI25K could realize the complete gel retardation of siRNA and DOX-Duplex at a mass ratio of 1.0, and it could simultaneously condense these two components at mass ratios of 1:1:1 and 2:1:1 to form stable nanocomplexes. Furthermore, the carrier PEI25K could protect the cargos from the degradation in the presence of 50% FBS, no matter for the single cargo loading and the co-delivery system, in which 4 mg/mL heparin was used to destroy the nanocomplex

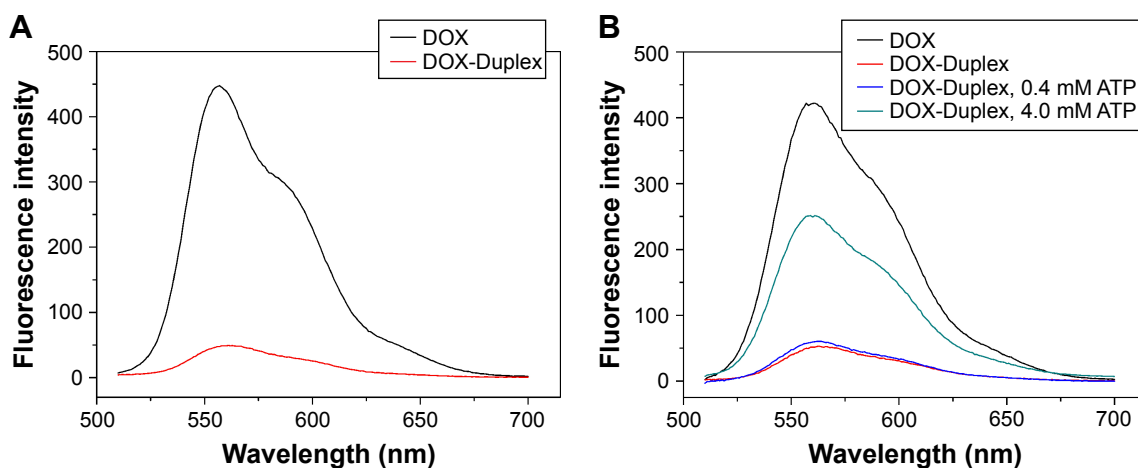


**Figure 1** Fluorescence spectra of DOX and DOX-Duplex (A) and ATP-triggered DOX release from DOX-Duplex through the incubation at different concentrations of ATP (0, 0.4 and 4.0 mM) for 15 min (B).

**Abbreviations:** DOX, doxorubicin; ATP, adenosine triphosphate.

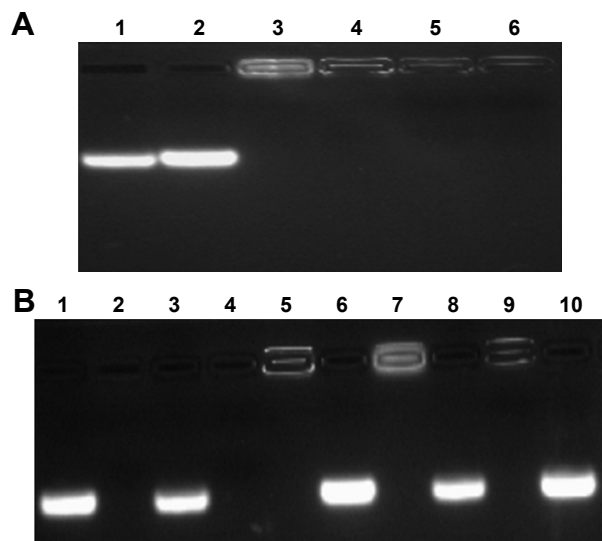


**Figure 2** Agarose gel electrophoresis for the condensation ability of PEI25K toward Bcl-2 siRNA and DOX-Duplex (**A**) and the stability of nanocomplex in the presence of 50% FBS (**B**).

**Notes:** (**A**) Lane 1: DOX-Duplex, lane 2: siRNA, lane 3: PEI/DOX-Duplex at a mass ratio of 1.0, lane 4: PEI/siRNA at a mass ratio of 1.0 and lanes 5 and 6: PEI/DOX-Duplex/siRNA at mass ratios of 1:1:1 and 2:1:1. (**B**) siRNA (lanes 1 and 2), DOX-Duplex (lanes 3 and 4), PEI25K/siRNA (mass ratio of 1.0, lanes 5 and 6), PEI25K/DOX-Duplex (mass ratio of 1.0, lanes 7 and 8) and PEI/DOX-Duplex/siRNA (mass ratio of 1:1:1, lanes 9 and 10) in the absence and presence of 50% FBS. The samples were pretreated with 4 mg/mL heparin before the agarose gel electrophoresis except for lanes 5, 7 and 9.

**Abbreviations:** DOX, doxorubicin; FBS, fetal bovine serum; PEI, polyethylenimine.

to release the oligonucleotides (Figure 2B). Owing to the loading of DOX, PEI25K could not condense the aptamer duplex as efficiently as Bcl-2 siRNA, which would lead to a much higher particle size of PEI/DOX-Duplex (Figure 3A). Nevertheless, the addition of Bcl-2 siRNA was beneficial for the binding and condensation of DOX-Duplex by PEI25K, achieving a particle size of 360.8 nm for the ternary nanocomplex PEI/DOX-Duplex/siRNA (mass ratio of 1:1:1). Meanwhile, the ternary nanocomplex exhibited a

positive state with zeta-potential of +9.85 mV (Figure 3B). These results demonstrated that the ternary nanocomplex was favorable for achieving an efficient cellular uptake and transfection efficiency. The fluorescence spectra of DOX release from PEI/DOX-Duplex and PEI/DOX-Duplex/siRNA after the treatment with 0.4 or 4.0 mM ATP showed that ATP could not trigger the cargo release from these delivery systems (Figure S1). These results demonstrated that PEI25K could efficiently condense DOX-Duplex and siRNA into stable nanocomplex and protect the cargo release. After the cellular uptake of nanoparticles, PEI25K could achieve the endosomal escape and rapid release of DOX-Duplex and siRNA through the proton sponge effect, and the released DOX-Duplex could rapidly release DOX molecules through the response to high ATP concentration in the cytosol. Meanwhile, PEI/DOX-Duplex/siRNA nanocomplex exhibited a weak ATP responsive ability in the ATP concentration of 0.4–4.0 mM (Figure S2). The cellular uptake of ternary nanocomplex PEI/DOX-Duplex/siRNA was then studied through its incubation with PC-3 cells for 6 h, in which DOX (red) and siRNA (green) could be obviously observed in the cells in a co-location manner (Figure 4). Meanwhile, the fluorescence intensity of DOX exhibited an increasing tendency with the elongation of incubation time (Figure 5), implying the gradual release of DOX in the intracellular environment. Additionally, the released DOX was specifically accumulated into the nuclei, which was consistent with previous research.<sup>20</sup> Combining the *in vitro* release analysis of DOX, the results elucidated that DOX could be successfully released from the duplex, which was probably caused by the transformational changes in duplex induced by the interaction between ATP aptamer and the high concentration of ATP in the cytosol.

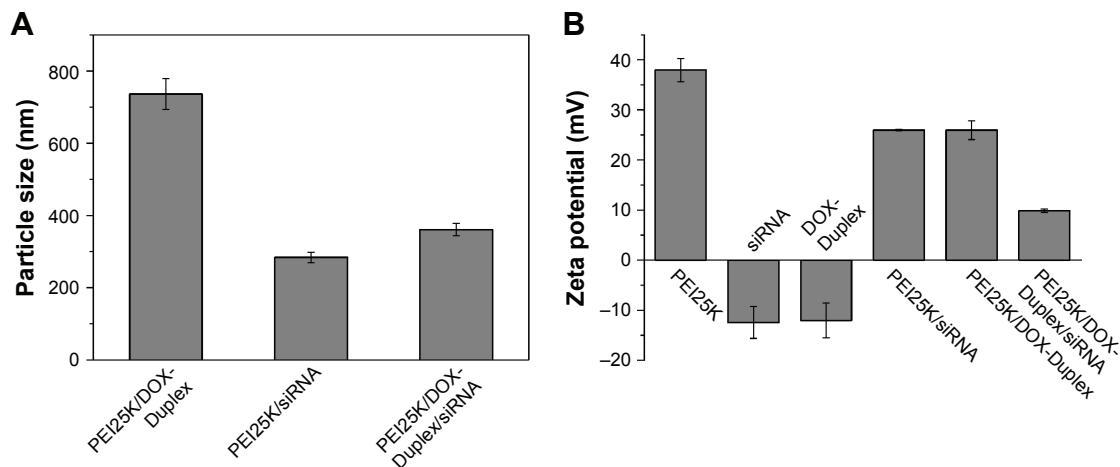


**Figure 3** Particle size (**A**) and zeta potential (**B**) of different nanocomplexes.

**Abbreviations:** PEI, polyethylenimine; DOX, doxorubicin.

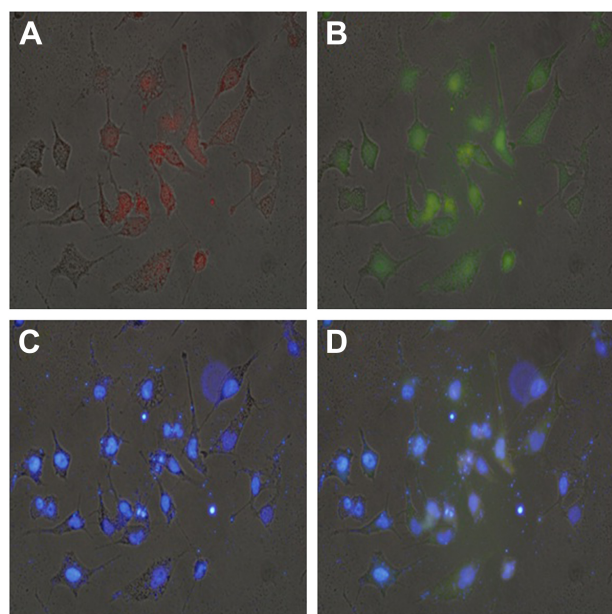


**Figure 4** The cellular uptake of ternary nanocomplex PEI/DOX-Duplex/siRNA for 6 h through fluorescence microscopic analysis.

**Notes:** (A) Red: DOX, (B) green: FAM-siRNA, (C) blue: DAPI for nuclei staining and (D) merge. Scale bar 50  $\mu$ m.

**Abbreviations:** PEI, polyethylenimine; DOX, doxorubicin; FAM, 5-carboxyfluorescein; DAPI, 4',6-diamidino-2-phenylindole.

To assay the anti-proliferation effect, the cell viabilities after the treatment with different nanocomplexes were measured through MTT. As shown in Figure 6, compared to the control, DOX-Duplex and PEI25K/siRNA exhibited almost no obvious effects on the cell proliferation with cell

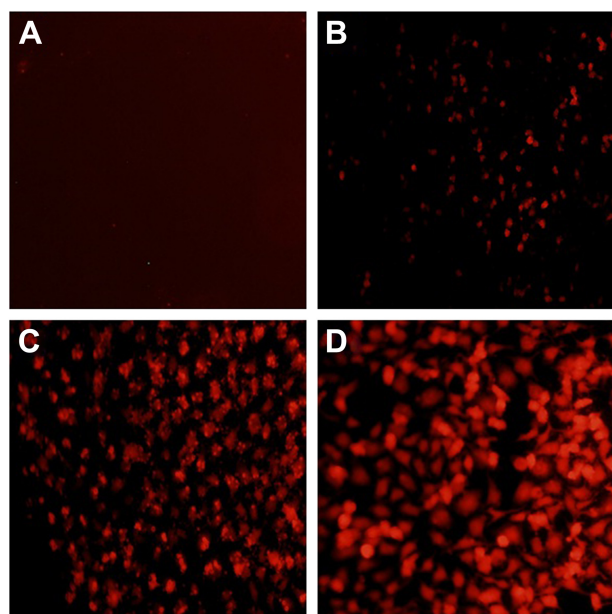


**Figure 5** The intracellular DOX release determined by fluorescence microscopy for 0 h (A), 6 h (B), 12 h (C) and 24 h (D). Scale bar 100  $\mu$ m.

**Abbreviation:** DOX, doxorubicin.

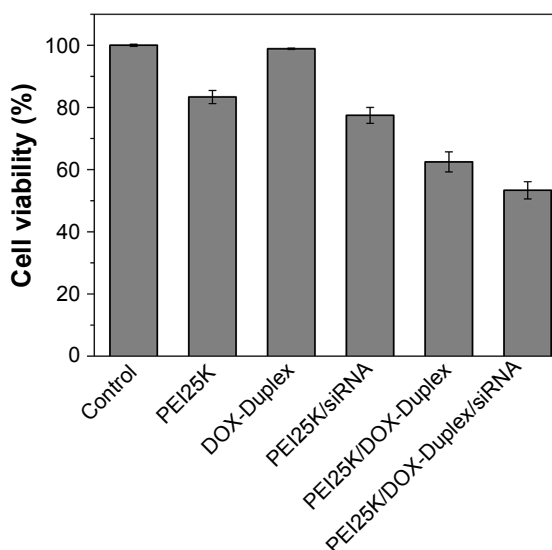


**Figure 6** Cell viabilities of PC-3 cells treated with different nanocomplexes for 24 h.

**Note:** Data were expressed as mean value  $\pm$  SD of three experiments.

**Abbreviations:** PEI, polyethylenimine; DOX, doxorubicin.

viability values of 98.9% and 77.5%, in which the latter was mainly caused by the cytotoxicity of PEI25K (cell viability of 83.3%). However, PEI25K-mediated delivery of DOX-Duplex could significantly inhibit the cell proliferation with cell viability of 62.5%, which was probably attributed to the efficient cellular uptake and subsequent DOX release quickly in the cytosol. Notably, the co-delivery system showed an enhanced induction of cell proliferation (cell viability of 53.3%), mainly owing to the synergistic anti-proliferative effect between these two components. Meanwhile, DOX-Duplex after the treatment with 4.0 mM ATP exhibited a similar inhibition effect to free DOX (Figure S3), indicating that the dissociation of aptamer duplex and subsequent DOX release could be achieved in an ATP-responsive manner. Through Western blot analysis, the expression level of Bcl-2 could be observed to be decreased after the treatment with PEI25K/siRNA and PEI/DOX-Duplex/siRNA (Figure 7).

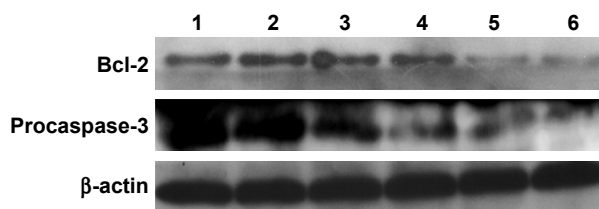


**Figure 7** Expression level of Bcl-2 and procaspase-3 in PC-3 cells after the treatment with different nanocomplexes for 24 h using Western blot: 1, control; 2, Bcl-2 siRNA; 3, DOX-Duplex; 4, PEI25K/DOX-Duplex; 5, PEI25K/siRNA and 6, PEI/DOX-Duplex/siRNA.

**Abbreviations:** DOX, doxorubicin; PEI, polyethylenimine.

The knockdown of Bcl-2 would contribute to the intrinsic inhibition of cell proliferation and even the reduction of anti-apoptotic defense,<sup>34</sup> which was promising for improving the antitumor efficacy of chemotherapeutics and decreasing the side effects through the reduced dosage, especially for solving the multidrug resistance of tumors. Live/Dead assay was conducted to evaluate the anti-proliferative effect of ternary nanocomplex, in which live and dead cells were stained green by the intracellular enzymatic hydrolysis of calcein AM and red by the intercalation of ethidium homodimer to DNA, respectively.<sup>35</sup> As shown in Figure 8, more death cells could be detected in PEI/DOX-Duplex/siRNA than in other groups. It was worthy to be noted that stronger induction of cell death could be achieved in the delivery of ternary nanocomplex than PEI25K/DOX-Duplex, implying the facilitated induction ability of cell death of Bcl-2 siRNA.

To get a deeper insight into the anti-proliferative mechanism, flow cytometry was conducted to monitor the cell apoptosis and cell-cycle arrest induced by the treatment of ternary nanocomplex. As shown in Figure 9, compared to the control group (3.97%), obvious early apoptosis could be achieved in PEI25K/siRNA and PEI25K/DOX-Duplex

groups, and meanwhile, PEI25K/DOX-Duplex exhibited a more powerful ability of inducing cell apoptosis (20.15%) than PEI25K/siRNA (7.88%). Surprisingly, the co-delivery of these two cargos showed a much stronger ability of inducing cell apoptosis than single cargos with an early apoptotic ratio of 36.23%. These results were consistent with the MTT assay, indicating the synergistic effect between DOX and Bcl-2 siRNA. Procaspase-3, the caspase-3's precursor, has been widely accepted to play a key role in the caspase family-related apoptotic cascade.<sup>36,37</sup> The expression level of procaspase-3 was dramatically decreased after the treatment with PEI/DOX-Duplex/siRNA (Figure 7), indicating the activation of caspase-3, which would subsequently catalyze the hydrolysis of many protein substrates for achieving the cell apoptosis. Furthermore, the treatment with PEI/DOX-Duplex/siRNA could obviously increase the activities of caspase-3 and caspase-9 and did not influence the caspase-8 activity (Figure 10). The caspase-9 can target procaspase-3 in the mitochondrial apoptosis pathway,<sup>38</sup> which meant the ternary nanocomplex PEI/DOX-Duplex/siRNA could activate the mitochondria-mediated pathway. However, the nanocarrier had no profound effects on death receptor-mediated pathway,

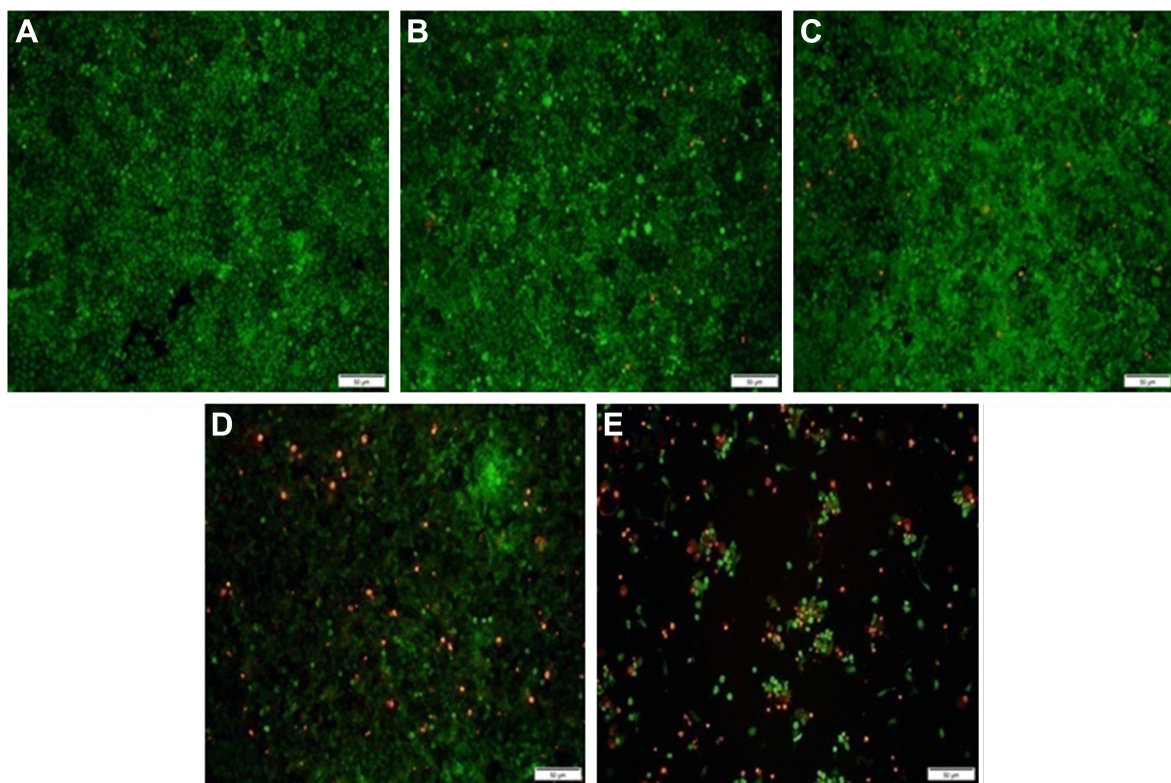


**Figure 8** Live/Dead assay of PC-3 cells treated with different nanocomplexes for 24 h: (A) control; (B) DOX-Duplex; (C) PEI25K/DOX-Duplex; (D) PEI25K/siRNA and (E) PEI/DOX-Duplex/siRNA.

**Notes:** The live and dead cells exhibited green and red fluorescence, respectively. Scale bar 200 µm.

**Abbreviations:** DOX, doxorubicin; PEI, polyethylenimine.

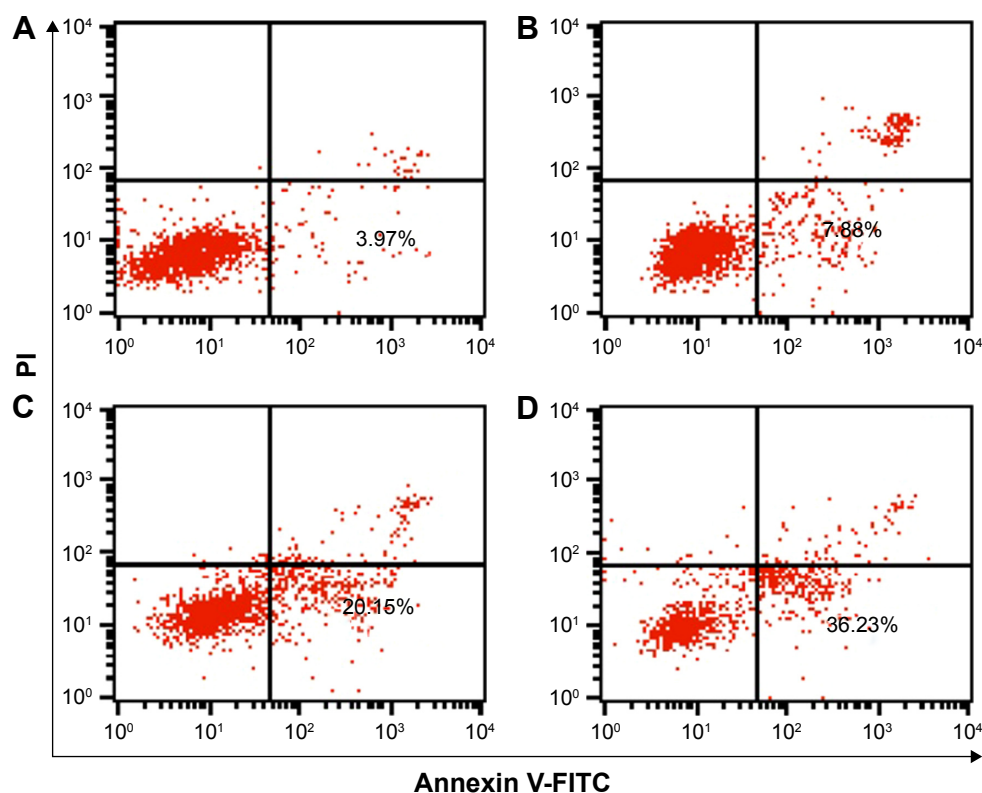


**Figure 9** Flow cytometric analysis of the cell apoptosis of PC-3 cells treated with different nanocomplexes for 24 h: (A) control, (B) PEI25K/siRNA, (C) PEI25K/DOX-Duplex and (D) PEI/DOX-Duplex/siRNA.

**Abbreviations:** PEI, polyethylenimine; DOX, doxorubicin; PI, propidium iodide; FITC, fluoresceine isothiocyanate.

in which caspase-8 possesses a death receptor domain and acts as an initiator caspase.<sup>38</sup> Similarly, more activation of caspase-3 and caspase-9 could be obtained in PEI/DOX-Duplex/siRNA than in other groups. Finally, cell-cycle arrest assay indicated that PEI25K/siRNA did not induce obvious cell-cycle arrest, while the ternary nanocomplex could improve

the G2 ratio (37.67%) and achieve the cell-cycle arrest at the G2 phase (Figure 11). Additionally, obvious sub-G1 phase could be observed in the PC-3 cells treated with DOX and Bcl-2 siRNA, which was a typical sign of cell apoptosis and consistent with the induction of cell apoptosis. Overall, our results elucidated that the enhanced anti-proliferative effect of ternary nanocomplex could be attributed to the induction of cell apoptosis and cell-cycle arrest in a synergistic manner of chemotherapy and gene therapy.

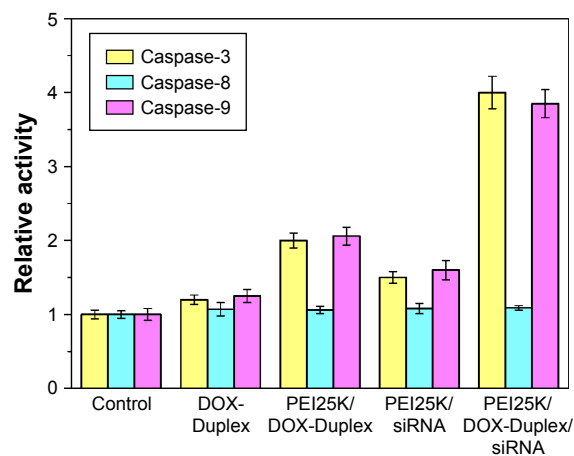


**Figure 10** Relative activity of caspase-3, -8 and -9 in PC-3 cells after the treatment with different nanocomplexes for 24 h.

**Abbreviations:** DOX, doxorubicin; PEI, polyethylenimine.

## Conclusion

Based on an ATP-responsive aptamer, a nanocarrier for co-delivering DOX and Bcl-2 siRNA has been successfully constructed. The ATP-triggered rapid release of cargos in the cytosol and the synergistic effect between these two cargos made it an ideal delivery system for achieving an efficient anti-proliferative effect through the induction of cell apoptosis and cell-cycle arrest. The strategy of combining chemotherapy and gene therapy in an ATP-responsive manner could potentially be used in the construction of smart delivery systems with favorable antitumor efficacy, especially for overcoming the multidrug resistance of tumors.



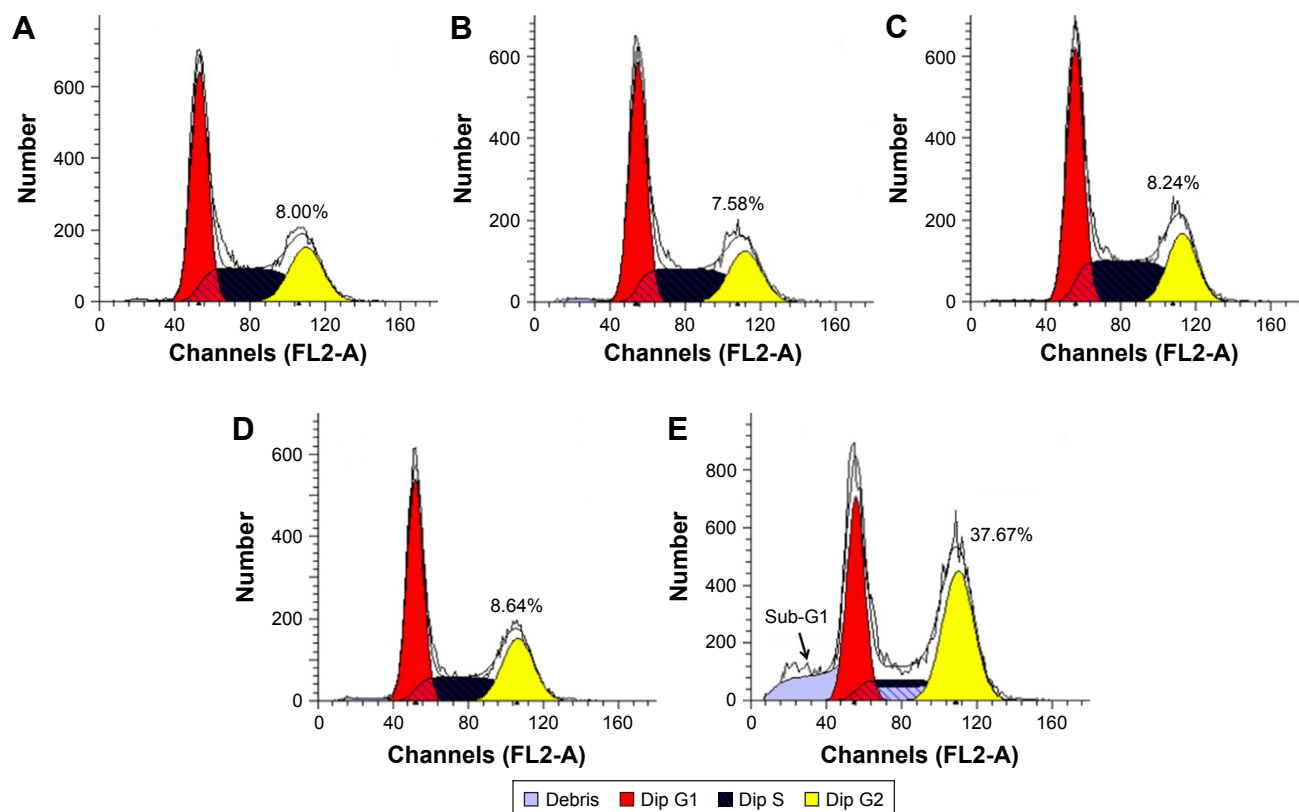


**Figure 11** Flow cytometric analysis of cell-cycle arrest in PC-3 cells after the treatment with different nanocomplexes for 24 h: (A) control, (B) siRNA, (C) DOX-Duplex, (D) PEI25K/siRNA and (E) PEI/DOX-Duplex/siRNA.

**Abbreviations:** DOX, doxorubicin; PEI, polyethylenimine.

## Acknowledgment

The authors gratefully acknowledge the financial supports from the Natural Science Foundation of China (Nos 81373344, 81473142, 81673502 and 51403074), Science & Technology Department of Jilin Province (Nos 20140101140JC, 20160520144JH and 20160520146JH), Education Department of Jilin Province (No 2015469), Youth Fund of Health and Family Planning Commission of Jilin Province (No 2013Q026) and Norman Bethune Program of Jilin University (Nos 2015324 and 2015423).

## Disclosure

The authors report no conflicts of interest in this work.

## References

- Gandhi NS, Tekade RK, Chougule MB. Nanocarrier mediated delivery of siRNA/miRNA in combination with chemotherapeutic agents for cancer therapy: current progress and advances. *J Control Release*. 2014;194:238–256.
- Gu Y, Li J, Li Y, et al. Nanomicelles loaded with doxorubicin and curcumin for alleviating multidrug resistance in lung cancer. *Int J Nanomedicine*. 2016;11:5757–5770.
- Kachalaki S, Ebrahimi M, Mohamed Khosroshahi L, Mohammadinejad S, Baradaran B. Cancer chemoresistance; biochemical and molecular aspects: a brief overview. *Eur J Pharm Sci*. 2016;89:20–30.
- Pakunlu RI, Wang Y, Tsao W, Pozharov V, Cook TJ, Minko T. Enhancement of the efficacy of chemotherapy for lung cancer by simultaneous suppression of multidrug resistance and antiapoptotic cellular defense: novel multicomponent delivery system. *Cancer Res*. 2004;64(17):6214–6224.
- Leslie EM, Deeley RG, Cole SP. Multidrug resistance proteins: role of P-glycoprotein, MRP1, MRP2, and BCRP (ABCG2) in tissue defense. *Toxicol Appl Pharmacol*. 2005;204(3):216–237.
- Kapse-Mistry S, Govender T, Srivastava R, Yergeri M. Nanodrug delivery in reversing multidrug resistance in cancer cells. *Front Pharmacol*. 2014;5:159.
- Wu D, Wang C, Yang J, et al. Improving the intracellular drug concentration in lung cancer treatment through the codelivery of doxorubicin and miR-519c mediated by porous PLGA microparticle. *Mol Pharm*. 2016;13(11):3925–3933.
- Tsouris V, Joo MK, Kim SH, Kwon IC, Won YY. Nano carriers that enable co-delivery of chemotherapy and RNAi agents for treatment of drug-resistant cancers. *Biotechnol Adv*. 2014;32(5):1037–1050.
- Ling G, Zhang T, Zhang P, Sun J, He Z. Synergistic and complete reversal of the multidrug resistance of mitoxantrone hydrochloride by three-in-one multifunctional lipid-sodium glycocholate nanocarriers based on simultaneous BCRP and Bcl-2 inhibition. *Int J Nanomedicine*. 2016;11:4077–4091.
- Saad M, Garbuzenko OB, Minko T. Co-delivery of siRNA and an anti-cancer drug for treatment of multidrug-resistant cancer. *Nanomedicine*. 2008;3(6):761–776.

11. Walensky LD. BCL-2 in the crosshairs: tipping the balance of life and death. *Cell Death Differ*. 2006;13(8):1339–1350.
12. Wu D, Yang J, Xing Z, et al. Phenylboronic acid-functionalized polyamidoamine-mediated Bcl-2 siRNA delivery for inhibiting the cell proliferation. *Colloids Surf B Biointerfaces*. 2016;146:318–325.
13. Beh CW, Seow WY, Wang Y, et al. Efficient delivery of Bcl-2-targeted siRNA using cationic polymer nanoparticles: downregulating mRNA expression level and sensitizing cancer cells to anticancer drug. *Biomacromolecules*. 2009;10(1):41–48.
14. Hu CM, Zhang L. Nanoparticle-based combination therapy toward overcoming drug resistance in cancer. *Biochem Pharmacol*. 2012;83(8):1104–1111.
15. Li J, Wang Y, Zhu Y, Oupický D. Recent advances in delivery of drug-nucleic acid combinations for cancer treatment. *J Control Release*. 2013;172(2):589–600.
16. Xue W, Dahlman JE, Tammela T, et al. Small RNA combination therapy for lung cancer. *Proc Natl Acad Sci U S A*. 2014;111(34):3553–3561.
17. Wu D, Han H, Xing Z, et al. Ideal and reality: barricade in the delivery of small interfering RNA for cancer therapy. *Curr Pharm Biotechnol*. 2016;17(3):237–247.
18. Creixell M, Peppas NA. Co-delivery of siRNA and therapeutic agents using nanocarriers to overcome cancer resistance. *Nano Today*. 2012;7:367–379.
19. Rapoport N. Physical stimuli-responsive polymeric micelles for anticancer drug delivery. *Prog Polym Sci*. 2007;32:962–990.
20. Mo R, Jiang T, DiSanto R, Tai W, Gu Z. ATP-triggered anticancer drug delivery. *Nat Commun*. 2014;5:3364.
21. Wang G, Huang G, Zhao Y, et al. ATP triggered drug release and DNA co-delivery systems based on ATP responsive aptamers and polyethylenimine complexes. *J Mater Chem B*. 2016;4:3832–3841.
22. He X, Zhao Y, He D, Wang K, Xu F, Tang J. ATP-responsive controlled release system using aptamer-functionalized mesoporous silica nanoparticles. *Langmuir*. 2012;28(35):12909–12915.
23. Mo R, Jiang T, Sun W, Gu Z. ATP-responsive DNA-graphene hybrid nanoaggregates for anticancer drug delivery. *Biomaterials*. 2015;50:67–74.
24. Zhu X, Zhang B, Ye Z, Shi H, Shen Y, Li G. An ATP-responsive smart gate fabricated with a graphene oxide-aptamer-nanochannel architecture. *Chem Commun*. 2015;51(4):640–643.
25. Liao WC, Sohn YS, Riutin M, et al. The application of stimuli-responsive VEGF- and ATP-aptamer-based microcapsules for the controlled release of an anticancer drug, and the selective targeted cytotoxicity toward cancer cells. *Adv Funct Mater*. 2016;26:4262–4273.
26. Zhao P, Zheng M, Luo Z, et al. Oxygen nanocarrier for combined cancer therapy: oxygen-boosted ATP-responsive chemotherapy with amplified ROS lethality. *Adv Healthc Mater*. 2016;5(17):2161–2167.
27. Zhang Y, Lu Y, Wang F, et al. ATP/pH dual responsive nanoparticle with d-[des-Arg10]kallidin mediated efficient in vivo targeting drug delivery. *Small*. 2017;13(3):1602494.
28. Gribble FM, Loussouarn G, Tucker SJ, Zhao C, Nichols CG, Ashcroft FM. A novel method for measurement of submembrane ATP concentration. *J Biol Chem*. 2000;275(39):30046–30049.
29. Gorman MW, Feigl EO, Buffington CW. Human plasma ATP concentration. *Clin Chem*. 2007;53(2):318–325.
30. Kim D, Jeong YY, Jon S. A drug-loaded aptamer-gold nanoparticle bioconjugate for combined CT imaging and therapy of prostate cancer. *ACS Nano*. 2010;4(7):3689–3696.
31. Xiao Z, Ji C, Shi J, et al. DNA self-assembly of targeted near-infrared-responsive gold nanoparticles for cancer thermo-chemotherapy. *Angew Chem Int Ed*. 2012;51:11853–11857.
32. Godbey WT, Wu KK, Mikos AG. Tracking the intracellular path of poly(ethylenimine)/DNA complexes for gene delivery. *Proc Natl Acad Sci U S A*. 1999;96(9):5177–5181.
33. Tian H, Lin L, Chen J, Chen X, Park TG, Maruyama A. RGD targeting hyaluronic acid coating system for PEI-PBLG polycation gene carriers. *J Control Release*. 2011;155(1):47–53.
34. Taghavi S, Hashemnia A, Mosaffa F, Askarian S, Abnous K, Ramezani M. Preparation and evaluation of polyethylenimine-functionalized carbon nanotubes tagged with 5TR1 aptamer for targeted delivery of Bcl-xL shRNA into breast cancer cells. *Colloids Surf B Biointerfaces*. 2016;140:28–39.
35. Tanaka A, Fukuoka Y, Morimoto Y, et al. Cancer cell death induced by the intracellular self-assembly of an enzyme-responsive supramolecular gelator. *J Am Chem Soc*. 2015;137(2):770–775.
36. Yang TJ, Haimovitz-Friedman A, Verheij M. Anticancer therapy and apoptosis imaging. *Exp Oncol*. 2012;34(3):269–276.
37. Zhang J, Wu D, Xing Z, et al. N-Isopropylacrylamide-modified polyethylenimine-mediated p53 gene delivery to prevent the proliferation of cancer cells. *Colloids Surf B Biointerfaces*. 2015;129:54–62.
38. Kiraz Y, Adan A, Kartal MY, et al. Major apoptotic mechanisms and genes involved in apoptosis. *Tumour Biol*. 2016;37:8471–8486.

## Supplementary materials

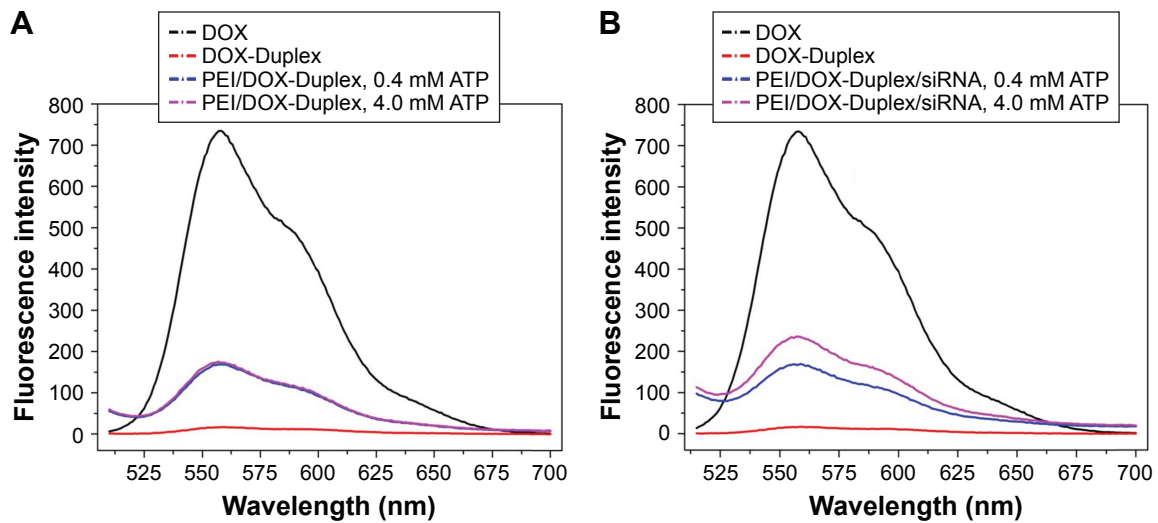


**Figure S1** Fluorescence spectra of DOX release from PEI/DOX-Duplex (A) and PEI/DOX-Duplex/siRNA (B) through the incubation at different concentrations of ATP (0.4 and 4.0 mM) for 15 min.

**Abbreviations:** DOX, doxorubicin; PEI, polyethylenimine; ATP, adenosine triphosphate.

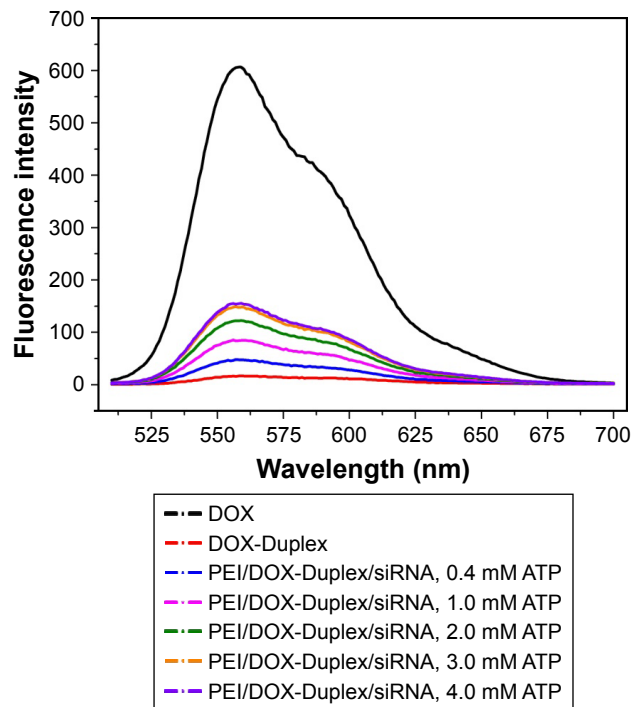


**Figure S2** Fluorescence spectra of DOX release from PEI/DOX-Duplex/siRNA through the incubation at different concentrations of ATP (0.4–4.0 mM) for 15 min.

**Abbreviations:** DOX, doxorubicin; PEI, polyethylenimine; ATP, adenosine triphosphate.

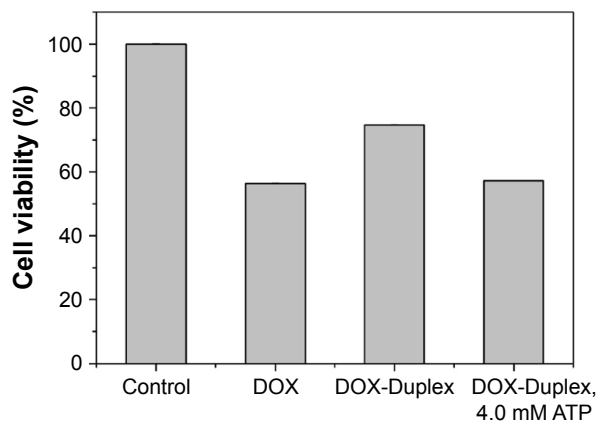


**Figure S3** Cell viabilities of PC-3 cells treated with free DOX (0.5  $\mu$ M) and DOX-Duplex for 48 h.

**Note:** Data were expressed as mean value  $\pm$  SD of three experiments.

**Abbreviations:** DOX, doxorubicin; ATP, adenosine triphosphate.

International Journal of Nanomedicine

Dovepress

### Publish your work in this journal

The International Journal of Nanomedicine is an international, peer-reviewed journal focusing on the application of nanotechnology in diagnostics, therapeutics, and drug delivery systems throughout the biomedical field. This journal is indexed on PubMed Central, MedLine, CAS, SciSearch®, Current Contents®/Clinical Medicine,

Journal Citation Reports/Science Edition, EMBase, Scopus and the Elsevier Bibliographic databases. The manuscript management system is completely online and includes a very quick and fair peer-review system, which is all easy to use. Visit <http://www.dovepress.com/testimonials.php> to read real quotes from published authors.

Submit your manuscript here: <http://www.dovepress.com/international-journal-of-nanomedicine-journal>